Electronic Supplementary Material (ESI) for Materials Horizons.

— Electronic Supplementary Information —

Computational Design of Thermoelectric Alloys Through Optimization of Transport and Dopability

Jiaxing Qu,[†] Adam Balvanz,[‡] Sviatoslav Baranets,[‡] Svilen Bobev,[‡] and Prashun Gorai*[,¶]

[†]*University of Illinois at Urbana-Champaign, Urbana, IL 61801*

[‡]*University of Delaware, Newark, DE 19716*

[¶]*Colorado School of Mines, Golden, CO 80401*

E-mail: pgorai@mines.edu

1. Atomic Coordinates and Equivalent Displacement Parameters

Table S1: Fractional atomic coordinates and equivalent displacement parameters (Å^2) for (1) $Sr_2CdP_2^*$ and (2) the Ba-poor compositions of the solid solution $Ba_{2(1-x)}Sr_{2x}CdP_2$.
*Sr_2CdP_2 was not resynthesized in this study, but is presented for reference. For information on Sr_2CdP_2, please see our previous work.[1] † U_{eq} is defined as one third of the trace of the orthogonalized U_{ij} tensor.

Composition	x	y	z	$U_{eq}^{\dagger}$
Sr_2CdP_2				
Sr1	0	0.29673 (9)	0.5970 (2)	0.0143 (4)
Sr2	0	0.46350 (1)	0.2560 (2)	0.0129 (4)
Cd	0	0.09625 (7)	0.4103 (2)	0.0136 (3)
P1	0	0.06150 (3)	0.0518 (6)	0.0116 (9)
P2	0	0.32570 (3)	0.0000 (7)	0.0130 (1)
$Ba_{0.4}Sr_{1.6}CdP_2$				
Ba1/Sr1	0	0.29689 (4)	0.5944 (1)	0.0150 (3)
Sr2	0	0.46517 (6)	0.2601 (1)	0.0125 (2)
Cd	0	0.09531 (4)	0.41551 (9)	0.0138 (2)
P1	0	0.0598 (2)	0.0549 (4)	0.0116 (6)
P2	0	0.3283 (2)	0.0058 (4)	0.0137 (6)
$Ba_{0.6}Sr_{1.4}CdP_2$				
Ba1/Sr1	0	0.29707 (4)	0.5927 (1)	0.0137 (3)
Sr2	0	0.46568 (7)	0.2608 (2)	0.0112 (2)
Cd	0	0.09491 (5)	0.41614 (9)	0.0126 (2)
P1	0	0.0593 (2)	0.0556 (4)	0.0109 (6)
P2	0	0.3294 (2)	0.0066 (4)	0.0139 (7)
$Ba_{0.7}Sr_{1.3}CdP_2$				
Ba1/Sr1	0	0.29717 (3)	0.5903 (1)	0.0112 (2)
Sr2	0	0.46632 (5)	0.2607 (2)	0.0092 (2)
Cd	0	0.09454 (4)	0.41671 (9)	0.0107 (2)
P1	0	0.0585 (2)	0.0556 (4)	0.0089 (5)
P2	0	0.3304 (2)	0.0074 (4)	0.0115 (6)
$Ba_{0.9}Sr_{1.1}CdP_2$				
Ba1/Sr1	0	0.29721 (5)	0.5891 (1)	0.0110 (3)
Ba2/Sr2	0	0.46658 (8)	0.2619 (2)	0.0093 (4)
Cd	0	0.09403 (5)	0.4180 (1)	0.0102 (3)
P1	0	0.0577 (2)	0.0563 (5)	0.0096 (8)
P2	0	0.3318 (2)	0.0084 (5)	0.0115 (9)

Table S2: Fractional atomic coordinates and equivalent displacement parameters (Å^2) for (1) $Ba_2CdP_2^*$ and (2) the Ba-rich compositions of the solid solution $Ba_{2(1-x)}Sr_{2x}CdP_2$.
*Ba_2CdP_2 was not resynthesized in this study, but is presented for reference. For information on Ba_2CdP_2, please see our previous work.[1] † U_{eq} is defined as one third of the trace of the orthogonalized U_{ij} tensor.

Composition	x	y	z	$U_{eq}^{\dagger}$
$Ba_{1.1}Sr_{0.9}CdP_2$				
Ba1	0	0.29727 (3)	0.5897 (1)	0.0122 (2)
Ba2/Sr2	0	0.46636 (5)	0.2624 (1)	0.0100 (3)
Cd	0	0.09407 (4)	0.41837 (9)	0.0100 (2)
P1	0	0.0579 (1)	0.0573 (4)	0.0091 (5)
P2	0	0.3316 (2)	0.0084 (4)	0.0100 (6)
$Ba_{1.2}Sr_{0.8}CdP_2$				
Ba1	0	0.29723 (5)	0.5907 (2)	0.0148 (2)
Ba2/Sr2	0	0.46540 (7)	0.2629 (2)	0.0121 (4)
Cd	0	0.09397 (6)	0.4173 (1)	0.0127 (3)
P1	0	0.0582 (2)	0.0585 (6)	0.0123 (8)
P2	0	0.3315 (2)	0.0058 (6)	0.016 (1)
$Ba_{1.3}Sr_{0.7}CdP_2$				
Ba1	0	0.29682 (4)	0.5925 (1)	0.0137 (2)
Ba2/Sr2	0	0.46432 (6)	0.2626 (1)	0.0110 (3)
Cd	0	0.09418 (5)	0.4162 (1)	0.0113 (2)
P1	0	0.0578 (2)	0.0598 (4)	0.0103 (6)
P2	0	0.3308 (2)	0.0035 (4)	0.0126 (7)
$Ba_{1.6}Sr_{0.4}CdP_2$				
Ba1	0	0.29650 (3)	0.59502 (9)	0.0130 (1)
Ba2/Sr2	0	0.46206 (4)	0.26294 (9)	0.0102 (2)
Cd	0	0.09428 (4)	0.41371 (8)	0.0114 (2)
P1	0	0.0581 (1)	0.0620 (3)	0.0100 (5)
P2	0	0.3304 (2)	-0.0030 (3)	0.0127 (6)
Ba_2CdP_2				
Ba1	0	0.29615 (6)	0.6105 (1)	0.0136 (2)
Ba2	0	0.45930 (6)	0.2754 (1)	0.0128 (2)
Cd	0	0.09480 (7)	0.4223 (2)	0.0140 (3)
P1	0	0.0585 (3)	0.0775 (6)	0.0124 (9)
P2	0	0.3287 (3)	0.0000 (6)	0.012 (1)

2. Selected Bond Distances for $Ba_{2(1-x)}Sr_{2x}CdP_2$

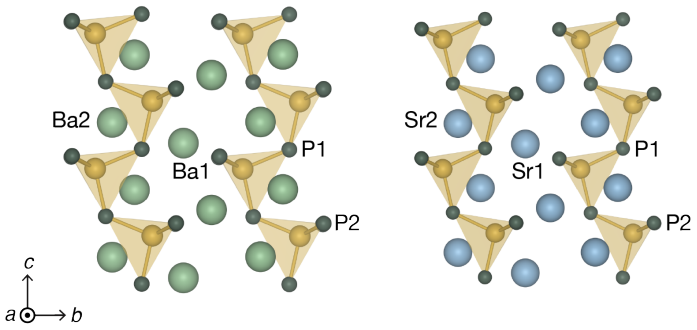

Figure S1: Crystal structures of Ba_2CdP_2 and Sr_2CdP_2 with labels for different Wyckoff sites of Ba, Sr, and P.

Table S3: Selected bond distances (Å).

Composition	**Ba1/Sr1-P1 Distance (Å)**	**Ba1/Sr1-P2 Distance (Å)**
$Ba_{0.4}Sr_{1.6}CdP_2$	3.264(3)×2	3.104(3)×2
$Ba_{0.6}Sr_{1.4}CdP_2$	3.284(3)×2	3.126(3)×2
$Ba_{0.7}Sr_{1.3}CdP_2$	3.303(2)×2	3.148(2)×2
$Ba_{0.9}Sr_{1.1}CdP_2$	3.332(3)×2	3.180(3)×2
$Ba_{1.1}Sr_{0.9}CdP_2$	3.331(2)×2	3.182(2)×2
$Ba_{1.2}Sr_{0.8}CdP_2$	3.329(3)×2	3.188(3)×2
$Ba_{1.3}Sr_{0.7}CdP_2$	3.338(2)×2	3.181(2)×2
$Ba_{1.6}Sr_{0.4}CdP_2$	3.3416(18)×2	3.1943(19)×2

3. Selected Bond Angles for $Ba_{2(1-x)}Sr_{2x}CdP_2$

Table S4: Selected bond angles.

Composition	**P1-Cd1-P1 angle (°)**	**Cd-P1-Cd angle (°)**
$Ba_{0.4}Sr_{1.6}CdP_2$	99.21 (7)	124.24 (9)
$Ba_{0.6}Sr_{1.4}CdP_2$	99.03 (8)	124.36 (12)
$Ba_{0.7}Sr_{1.3}CdP_2$	98.81 (5)	124.48 (10)
$Ba_{0.9}Sr_{1.1}CdP_2$	98.68 (8)	124.65 (13)
$Ba_{1.1}Sr_{0.9}CdP_2$	98.80 (5)	124.67 (10)
$Ba_{1.2}Sr_{0.8}CdP_2$	99.38 (8)	124.96 (15)
$Ba_{1.3}Sr_{0.7}CdP_2$	99.79 (6)	125.71 (11)
$Ba_{1.6}Sr_{0.4}CdP_2$	100.95 (5)	126.59 (9)

4. Crystallographic and Refinement Parameters for Ba-Poor Compositions

Table S5: Crystallographic and refinement parameters for the Ba-poor compositions of $Ba_{2(1-x)}Sr_{2x}CdP_2$.

Composition	**$Sr_2CdP_2^*$**	**$Ba_{0.4}Sr_{1.6}CdP_2$**	**$Ba_{0.6}Sr_{1.4}CdP_2$**	**$Ba_{0.6}Sr_{1.4}CdP_2$**	**$Ba_{0.7}Sr_{1.3}CdP_2$**	**$Ba_{0.9}Sr_{1.1}CdP_2$**
CCDC	2034151	2107428	2107429	2107430	2107431	2107432
Site 1 Ba/Sr ratio	Sr only	0.41(1)/0.59(1)	0.56(1)/0.44(1)	0.61(1)/0.39(1)	0.70(1)/0.30(1)	0.90(1)/0.10(1)
Site 2 Ba/Sr ratio	Sr only	Sr only	Sr only	Sr only	Sr only	0.04(1)/0.96(1)
Formula Weight (g/mol)	349.58	369.84	377.30	379.91	384.38	369.19
Z	4					
Temp. (K)	200(1)					
Radiation Source, λ	Mo K_α, 0.71073 Å					
Space Group	$Cmc2_1$ (No. 36)					
a (Å)	4.325 (18)	4.369 (3)	4.377 (3)	4.380 (3)	4.392 (2)	4.411(8)
b (Å)	16.506 (7)	16.800 (10)	16.921 (13)	16.932 (11)	17.010 (10)	17.132 (3)
c (Å)	7.469 (3)	7.450 (5)	7.447 (6)	7.443 (5)	7.443 (4)	7.463 (15)
V (Å^3)	533.2 (4)	546.9 (6)	551.6 (7)	551.99 (6)	555.94(5)	563.9 (2)
ρ_{calc} (g/cm^3)	4.354	4.492	4.543	4.571	4.592	4.666
μ (cm^{-1})	243.04	226.41	220.61	219.09	215.24	206.20
Goodness-of fit	0.994	1.033	0.869	1.081	1.060	0.905
R_1 ($I > 2\sigma_I$)†	0.0392	0.0271	0.0250	0.0242	0.0221	0.0321
R_1 (all data)	0.0459	0.0281	0.0267	0.0256	0.0230	0.0387
wR_2 ($I > 2\sigma_I$)^2	0.0664	0.0568	0.0460	0.0415	0.0550	0.0427
wR_2 (all data)	0.0682	0.0571	0.0464	0.0419	0.0555	0.0445
Largest Peak (e$^-$/Å^3)	1.60	0.94	0.91	0.95	0.88	1.21
Deepest Hole (e$^-$/Å^3)	-1.10	-1.18	-1.70	-1.03	-0.85	-1.56

*Sr_2CdP_2 was not resynthesized for this study. Instead, the crystallographic information and refinement parameters are listed from our previous work for reference.[1]

$^\dagger R_1 = \Sigma\big||F_o| - |F_c|\big| / \Sigma|F_o|$; $wR_2 = [\Sigma[w(F_o^2 - F_c^2)^2]/\Sigma[w(F_o^2)^2]]^{1/2}$, where $w = 1/[\sigma^2 F_o^2 + (AP)^2 + (BP)]$, and $P = (F_o^2 + 2F_c^2)/3$; A, B are the respective weight coefficients (found in the crystallographic information file (CIF))

Table S6: Crystallographic and refinement parameters for the Ba-rich compositions of $Ba_{2(1-x)}Sr_{2x}CdP_2$.

Formula	**$Ba_{1.1}Sr_{0.9}CdP_2$**	**$Ba_{1.1}Sr_{0.9}CdP_2$**	**$Ba_{1.2}Sr_{0.9}CdP_2$**	**$Ba_{1.3}Sr_{0.7}CdP_2$**	**$Ba_{1.6}Sr_{0.4}CdP_2$**	**$Ba_2CdP_2^*$**
CCDC	2107433	2107434	2107435	2107436	2107437	2034150
Site 1 Ba/Sr ratio	Ba only	Ba only	Ba only	Ba only	Ba only	Ba only
Site 2 Ba/Sr ratio	0.11(8)/0.89(8)	0.10(1)/0.90(1)	0.19(1)/0.81(1)	0.32(7)/0.68(7)	0.57(5)/0.43(5)	Ba only
Formula Weight (g/mol)	404.77	404.27	408.75	415.33	427.64	449.02
Z			4			
Temp. (K)			200(1)			
Radiation Source, λ			Mo K_α, 0.71073 Å			
Space Group			$Cmc2_1$ (No. 36)			
a (Å)	4.416 (3)	4.416 (6)	4.422 (15)	4.428 (3)	4.446 (3)	4.473 (6)
b (Å)	17.140 (11)	17.154 (2)	17.132 (6)	17.101 (11)	17.065 (10)	17.105 (2)
c (Å)	7.474 (5)	7.468 (11)	7.524 (3)	7.588 (5)	7.722 (5)	7.924 (11)
V (Å^3)	565.6 (7)	565.7 (1)	570.0 (3)	574.5 (7)	585.8 (6)	603.1 (1)
ρ_{calc} (g/cm^3)	4.753	4.747	4.763	4.802	4.848	6.114
μ (cm^{-1})	201.25	201.48	197.72	192.89	183.16	167.79
Goodness-of fit	1.049	1.090	1.038	1.064	1.086	0.988
R_1 (I>2σ_I)†	0.0212	0.0261	0.0320	0.0267	0.0191	0.0349
R_1 (all data)	0.0223	0.0272	0.0342	0.0290	0.0195	0.0392
wR_2 (I>2σ_I)^2	0.0458	0.0540	0.0568	0.0448	0.0339	0.0594
wR_2 (all data)	0.0462	0.0546	0.0576	0.0457	0.0340	0.0606
Largest Peak (e$^-$/Å^3)	1.13	0.76	1.27	1.01	0.89	1.53
Deepest Hole (e$^-$/Å^3)	-1.35	-0.88	-1.70	-1.47	-1.34	-1.40

* Ba_2CdP_2 was not resynthesized for this inquiry. Instead, the crystallographic information and refinement parameters are listed from our previous work for reference.[1]

$^\dagger R_1 = \Sigma\big||F_o| - |F_c|\big| / \Sigma|F_o|$; $wR_2 = [\Sigma[w(F_o^2 - F_c^2)^2]/\Sigma[w(F_o^2)^2]]^{1/2}$, where $w = 1/[\sigma^2 F_o^2 + (AP)^2 + (BP)]$, and $P = (F_o^2 + 2F_c^2)/3$; A, B are the respective weight coefficients (found in the crystallographic information file (CIF))

5. Convergence Test for SQS Used to Calculate Effective Band Structure

Table S7: Comparison of the electronic structure properties of 100- and 200-atom SQS supercells of $Ba_{0.4}Sr_{1.6}CdP_2$ ($x = 0.8$). The band gap (E_g), valence band density-of-states effective mass ($m^*_{\mathrm{DOS,VB}}$), and conduction band density-of-states effective mass($m^*_{\mathrm{DOS,CB}}$) are found to be sufficiently converged for the 100-atom SQS. E_g, $m^*_{\mathrm{DOS,VB}}$, and $m^*_{\mathrm{DOS,CB}}$ are calculated from the effective band structures. The DOS effective mass is calculated within a 100 meV energy window from the relevant band edges, following the methodology reported in our previous works.[1,2]

size of SQS	E_g (eV)	$m^*_{\mathrm{DOS,VB}}$ (m_e)	$m^*_{\mathrm{DOS,CB}}$ (m_e)
100	0.872	0.43	0.05
200	0.872	0.31	0.06

6. Effective Band Structure of $Ba_{0.7}Sr_{1.3}CdP_2$ ($x = 0.65$)

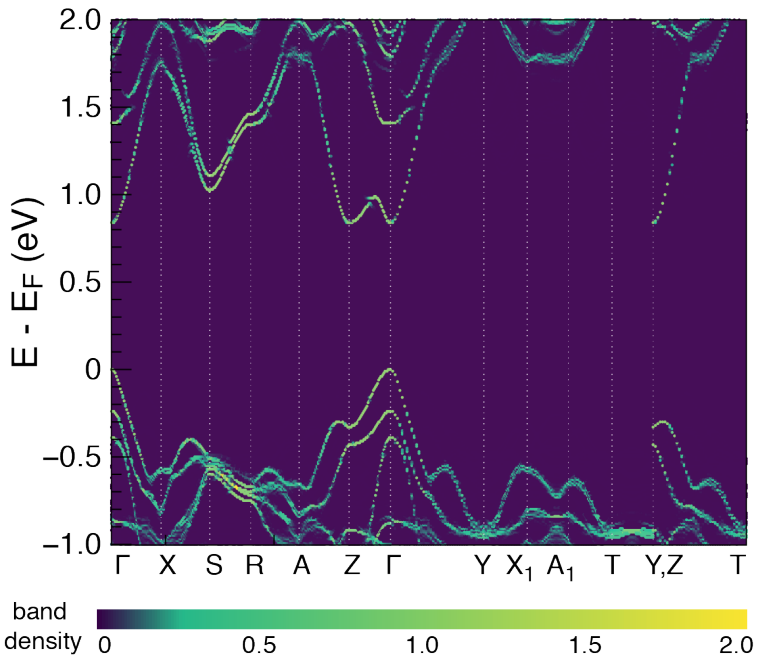

Figure S2: The effective band structure of $Ba_{0.7}Sr_{1.3}CdP_2$ ($x = 0.65$) alloy along special $\vec{k}$-point paths of the orthorhombic Brillouin zone.

7. Effect of Number of Interpolation Points on the EBS

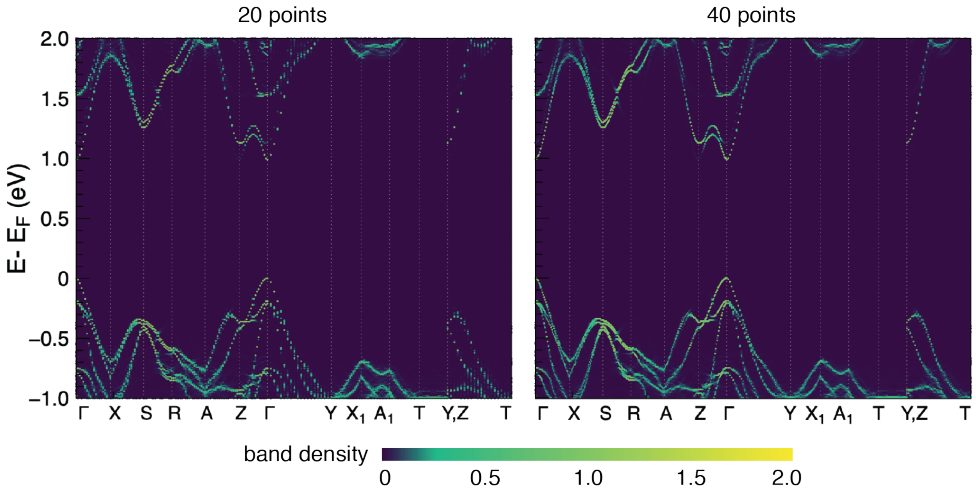

Figure S3: The effective band structure of $Ba_{0.4}Sr_{1.6}CdP_2$ ($x = 0.8$) calculated with two different number of interpolation points between each pair of high symmetry k-points of the primitive cell.

8. Atomic Sites in the Defect Supercell

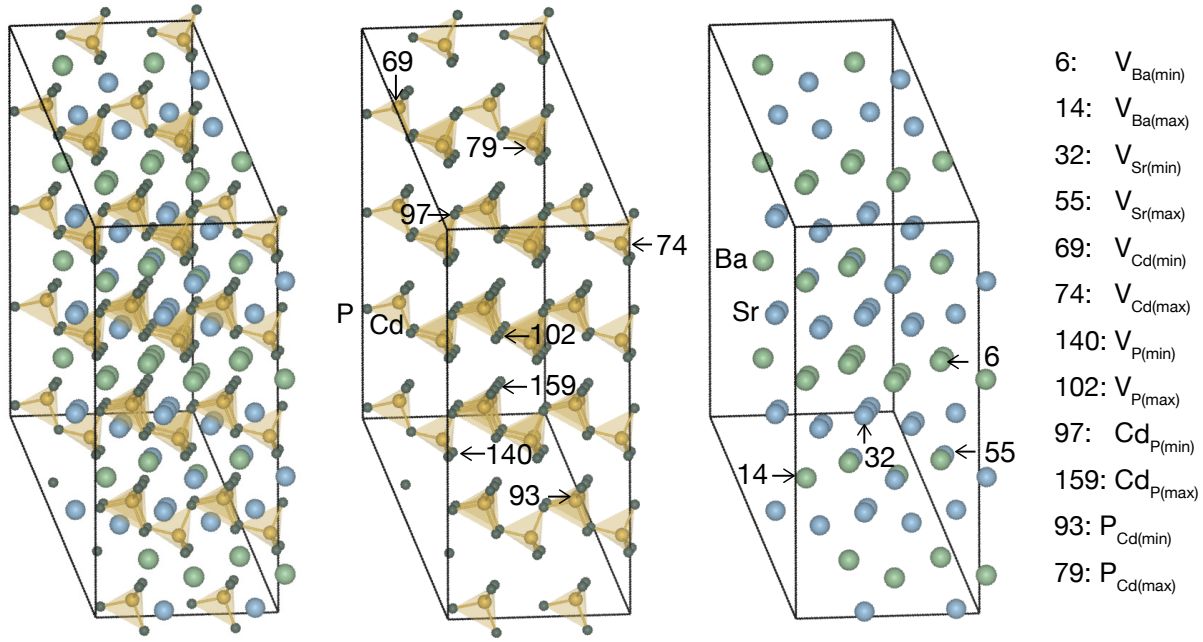

Figure S4: Crystal structures of 160-atom supercell of $Ba_{0.75}Sr_{1.25}CdP_2$ ($x = 0.625$) used in defect calculations. The atomic indices corresponding to the maximum and minimum $\Delta E_{D,q}$ for each defect in the neutral charge state (Figure 7a in the main text) are labeled.

9. Convergence Test for SQS Used in Defect Calculations

Table S8: Comparison of the electronic structure properties of 40- and 120-atom SQS supercells of $Ba_{0.75}Sr_{1.25}CdP_2$ ($x = 0.625$). The band gap (E_g) and energy offset of the conduction bands at Γ and Z ($\Delta E_{\Gamma-Z}$) are extracted from the EBS. The 40-atom SQS reproduces the electronic properties of the larger 120-atom SQS, and therefore, can be considered sufficiently converged.

# atoms in SQS	E_g (eV)	$\Delta E_{\Gamma-Z}$ (eV)
40	0.838	0.01
120	0.837	0.01

10. Phase Stability of $Ba_{0.75}Sr_{1.25}CdP_2$ in Chemical Potential Space

Table S9: Four-phase equilibrium regions of $Ba_{0.75}Sr_{1.25}CdP_2$ in the quaternary Ba-Sr-Cd-P chemical potential space. $\Delta\mu_X$ (X = Sr, Ba, Cd, P) are the deviations in the elemental chemical potential from the reference values (μ_X^0), which are listed in Table S10.

Corner	$\Delta\mu_{Sr}$ (eV)	$\Delta\mu_{Ba}$ (eV)	$\Delta\mu_{Cd}$ (eV)	$\Delta\mu_{P}$ (eV)	Phases in equilibrium with $Ba_{0.75}Sr_{1.25}CdP_2$
P-1	–1.040	–1.239	–0.086	–1.634	$SrCd_{11}$-$SrCd_2$-$Ba_{0.6}Sr_{1.4}CdP_2$
P-2	–1.040	–1.139	–0.086	–1.672	$SrCd_{11}$, $SrCd_2$, $Ba_{0.9}Sr_{1.1}CdP_2$
P-3	–1.822	–1.921	–0.015	–0.925	$SrCd_{11}$, $SrCd_2P_2$, $Ba_{0.9}Sr_{1.1}CdP_2$
P-4	–1.753	–1.952	–0.021	–0.953	$SrCd_2P_2$, $SrCd_{11}$, $Ba_{0.6}Sr_{1.2}CdP_2$
P-5	–0.367	–0.566	–0.049	–2.125	SrP, SrCd, $Ba_{0.6}Sr_{1.2}CdP_2$
P-6	–0.312	–0.439	–0.504	–2.180	Ba_4P_3, SrCd, SrP
P-7	–0.344	–0.443	–0.472	–2.174	Ba_4P_3, SrCd, $Ba_{0.9}Sr_{1.1}CdP_2$
P-8	–1.790	–1.889	–0.524	–0.702	Sr_3P_4, SrP, $Ba_{0.9}Sr_{1.1}CdP_2$
P-9	–0.422	–0.521	–0.524	–2.070	Ba_4P_3, SrP, $Ba_{0.9}Sr_{1.1}CdP_2$
P-10	–1.790	–1.989	–0.449	–0.702	Sr_3P_4, SrP, $Ba_{0.6}Sr_{1.4}CdP_2$
P-11	–2.058	–2.157	–0.390	–0.501	Sr_3P_4, SrP_2, $Ba_{0.9}Sr_{1.1}CdP_2$
P-12	–2.072	–2.171	–0.376	–0.494	SrP_3, SrP_2, $Ba_{0.9}Sr_{1.1}CdP_2$
P-13	–2.051	–2.250	–0.319	–0.506	Sr_3P_4, $SrCd_2P_2$, $Ba_{0.6}Sr_{1.4}CdP_2$
P-14	–2.058	–2.250	–0.320	–0.501	Sr_3P_4, $SrCd_2P_2$, SrP_2
P-15	–2.072	–2.245	–0.320	–0.494	SrP_3, $SrCd_2P_2$, SrP_2
P-16	–2.120	–2.219	–0.313	–0.478	SrP_3, $SrCd_2P_2$, $Ba_{0.9}Sr_{1.1}CdP_2$
P-17	–0.421	–0.620	–0.395	–2.098	SrCd, $SrCd_2$, $Ba_{0.6}Sr_{1.4}CdP_2$
P-18	–0.421	–0.520	–0.395	–2.136	SrCd, $SrCd_2$, $Ba_{0.9}Sr_{1.1}CdP_2$

11. Reference Elemental Chemical Potentials

Table S10: Reference elemental chemical potentials.

Element	μ^0 (eV)
Sr	-4.11
Ba	-1.83
Cd	-0.88
P	-5.11

12. Free energy of mixing (ΔG_m) of ordered $BaSrCdP_2$

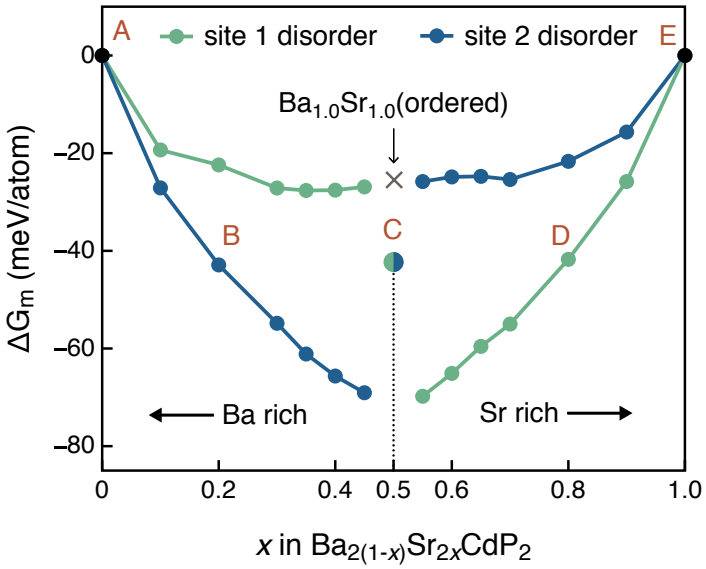

Figure S5: The free energy of mixing (ΔG_{m}) of ordered $BaSrCdP_2$,[1] where site 1 is fully occupied by Ba and site 2 by Sr (see Figure 2 in main text for definition of sites). ΔG_{m} of ordered $BaSrCdP_2$ (marked by $\times$) is smaller than that of disordered $BaSrCdP_2$ ($x = 0.5$), where both sites 1 and 2 are fully disordered. ΔG_{m} is calculated at 900 K, the typical synthesis temperature of $Ba_{2(1-x)}Sr_{2x}CdP_2$ alloys.

13. Free electron concentration for plausible n-type dopants in $Ba_{0.75}Sr_{1.25}CdP_2$

To evaluate n-type dopability of $Ba_{0.75}Sr_{1.25}CdP_2$ alloy, we calculate the free electron concentrations under three plausible extrinsic doping scenarios. We consider substitutional chalcogen doping on the P site, which will create singly-charged ($q = 1$) donor defects (assumed to be shallow). For each native defect, we consider the average defect formation energy (average of the maximum and minimum $\Delta E_{D,q}$ in Figure 7 in the main text). The average $\Delta E_{D,q}$ of V_{Cd} and V_P are shown as dotted lines in Figure S6. We simulate three different doping scenarios by adjusting $\Delta E_{D,q}$ at the conduction band minimum of the substitutional dopant. Namely, (A) $\Delta E_{D,q} = 0.29$ eV, (B) $\Delta E_{D,q} = 0.50$ eV, and (C) $\Delta E_{D,q} = 0.75$ eV, as shown in Figure S6. Scenarios (A), (B), and (C) correspond to no, moderate, and strong electron compensation by the holes formed due to native acceptor defect V_{Cd}. In each case, we find that $Ba_{0.75}Sr_{1.25}CdP_2$ is n-type with free electron concentrations of (A) 2.0×10^{19} cm^{-3}, (B) 4.4×10^{18} cm^{-3}, and (C) 7.6×10^{17} cm^{-3}.

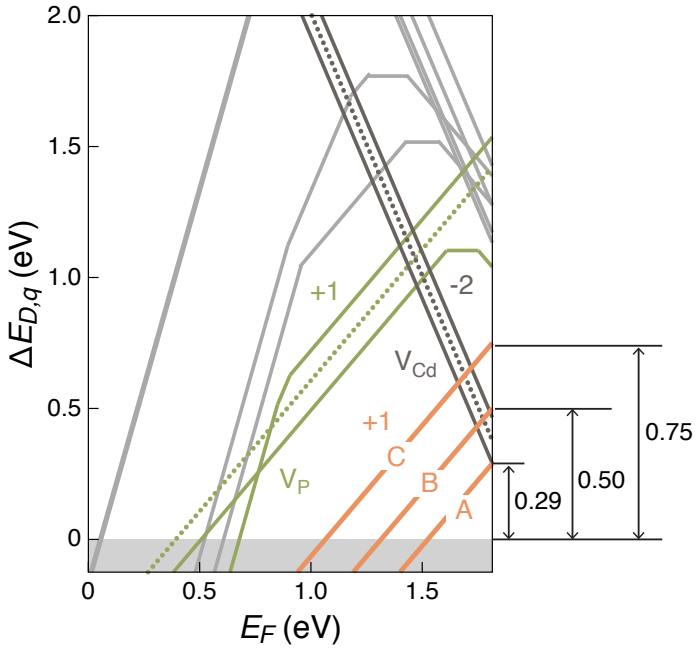

Figure S6: Defect formation energy of plausible n-type substitutional chalcogen dopants on the P site. Three doping scenarios are considered: (A) $\Delta E_{D,q} = 0.29$ eV, (B) $\Delta E_{D,q} = 0.50$ eV, and (C) $\Delta E_{D,q} = 0.75$ eV at the conduction band minimum.

References

(1) Balvanz, A.; Qu, J.; Baranets, S.; Ertekin, E.; Gorai, P.; Bobev, S. New n-Type Zintl Phases for Thermoelectrics: Discovery, Structural Characterization, and Band Engineering of the Compounds A_2CdP_2 (A = Sr, Ba, Eu). *Chem. Mater.* **2020**, *32*, 10697–10707.

(2) Yan, J.; Gorai, P.; Ortiz, B.; Miller, S.; Barnett, S. A.; Mason, T.; Stevanović, V.; Toberer, E. S. Material Descriptors for Predicting Thermoelectric Performance. *Energy Environ. Sci.* **2015**, *8*, 983.